Motion-Based Piloted Simulation Evaluation of a Control Allocation Technique to Recover from Pilot Induced Oscillations

Robert W. Craun[1]
Mission Critical Technologies, Inc., Moffett Field, California, 94035

Diana M. Acosta[2], Steven D. Beard[3]
NASA Ames Research Center, Moffett Field, California, 94035

Michael W. Leonard[4], Gordon H. Hardy[5], and Michael Weinstein[6],
Science Applications International Corporation, Moffett Field, California, 94035

and

Yildiray Yildiz[7]
University Affiliated Research Center, Moffett Field, California, 94035

This paper describes the maturation of a control allocation technique designed to assist pilots in the recovery from pilot induced oscillations (PIOs). The Control Allocation technique to recover from Pilot Induced Oscillations (CAPIO) is designed to enable next generation high efficiency aircraft designs. Energy efficient next generation aircraft require feedback control strategies that will enable lowering the actuator rate limit requirements for optimal airframe design. One of the common issues flying with actuator rate limits is PIOs caused by the phase lag between the pilot inputs and control surface response. CAPIO utilizes real-time optimization for control allocation to eliminate phase lag in the system caused by control surface rate limiting. System impacts of the control allocator were assessed through a piloted simulation evaluation of a non-linear aircraft simulation in the NASA Ames Vertical Motion Simulator. Results indicate that CAPIO helps reduce oscillatory behavior, including the severity and duration of PIOs, introduced by control surface rate limiting.

I. Introduction

TRENDS in Next Generation aircraft design relax stability requirements to gain improvements in energy efficiency and environmental compatibility through reduced drag. Stability refers to an aircraft's ability to passively return to an equilibrium state, typically original speed and orientation, after encountering a disturbance. Traditional transport aircraft are designed to be stable, but these design choices are the result of compromises in the bare airframe that degrade the aircraft's energy efficiency and environmental compatibility.[1,2] While studies[3,4,5,6]

---

[1] Former Aerospace Engineer, MCT, Inc, NASA Ames Research Center, Mail Stop 269-1. Currently Second Lieutenant in the United States Marine Corps.
[2] Aerospace Engineer, Intelligent Systems Division, Mail Stop 269-1.
[3] Simulation Engineer, Aerospace Simulation Research and Development Branch, Mail Stop 243-1, AIAA Senior Member.
[4] Former Senior Simulation Engineer, SAIC, NASA Ames Research Center, Mail Stop 243-6. Currently Senior Member of Consulting Staff, Mentor Graphics, Inc., 46871 Bayside Parkway, Fremont, California, 94538.
[5] Senior System Analyst, SAIC, NASA Ames Research Center, Mail Stop 243-6.
[6] Senior Simulation Engineer, SAIC, NASA Ames Research Center, Mail Stop 243-6.
[7] Associate Scientist, UARC, NASA Ames Research Center, Mail Stop 269-1, and AIAA Member.

have shown the fuel burn and emissions benefits of reduced stability or instability, work remains to ensure that the aircraft stability can be adequately augmented through feedback control systems. As the trend in aircraft design leads to marginally stable or unstable but controllable airframes, high control power and feedback control augmentation are required to improve flying qualities and maintain closed-loop stability. Of these two requirements, the high control power requirement poses a challenge for next generation transport and mobility aircraft.

Experience has shown that it is possible to stabilize unstable fighter aircraft with sufficient control power by using larger control surfaces and fast actuators. As the sizes of aircraft increase, the moment forces needed from the control surfaces also increases, resulting in the need for larger control surfaces. Moving these large control surfaces at a high rate required to meet stability and control demands will necessitate larger hydraulic systems with higher power requirements. These higher power requirements have been termed technologically challenging due to the unprecedented horsepower requirements.[5]

Control solutions are needed that will enable marginally stable and unstable airframe designs of next generation transport aircraft. These control solutions will involve the efficient use of many multi-axis control surfaces that are each designed at a minimum size such that together the surfaces provide sufficient control authority in each axis. Efficient use of the control surfaces will require balancing the available control authority in all axes while minimizing control surface deflections and rates. Research in recent years has begun to address these needs through the use of advanced control allocation techniques. Some of these include optimization methods for performance in the presence of control effector rate limits,[7] optimization methods for desired computational speed and implementation requirements,[8] investigations of the effects of control effector interactions for systems with many surfaces,[9] and minimization of control surface deflections to make more control power available as surfaces approach position saturation.[10] The Control Allocation technique to recover from Pilot Induced Oscillations (CAPIO) is one of the first known techniques to address the problems that arise from stringent actuator rate limits for multi-input, multi-output applications without the use of ganging.[11,12,13] In this paper, CAPIO is presented along with piloted simulation results of its effectiveness.

The objective of CAPIO is to enable energy efficient and environmentally compatible next generation aircraft with technologically achievable control surface rate limits. To do this, CAPIO seeks to allow aircraft to fly within a nominal flight envelope that includes cases when control surfaces are functioning at their rate limit. Traditionally, a nominal flight envelope will not include cases when control surfaces are functioning at their rate limits since this leads to phase lag associated with Pilot Induced Oscillations (PIO).[14] CAPIO actively detects and eliminates phase lag introduced by control surface rate limiting. By doings so, CAPIO allows the pilot to maintain or regain closed loop control of the aircraft.

This paper describes the maturation of CAPIO accomplished through a motion-based, piloted simulation evaluation. Specifically, the pilot-aircraft-control system was evaluated for demanding tasks and extreme aircraft configurations to observe the systems characteristics, including system performance, Handling Qualities ratings and Pilot Induced Oscillation ratings. Section II describes the PIO phenomenon and its link to Next Generation aircraft designs. This is followed in Section III by an overview of CAPIO as engineered to execute in real-time on the nonlinear aircraft simulation system. The simulation evaluation is described in Section IV, and Section V presents and discusses the results from the evaluation.

II. Pilot Induced Oscillation

A PIO is a sustained or uncontrollable, inadvertent oscillation resulting from the pilot's efforts to control the aircraft.[15] The pilot reacts to the motion of the aircraft, creating a closed-loop feedback control system. The oscillations can therefore be identified as closed-loop instabilities of a feedback control system.[16]

During a PIO, there are phase lags between the pilot's commands and the aircraft's responses. A typical PIO is characterized as "an oscillation at a frequency where the attitude response lags the stick inputs by approximately 180 degrees."[17] The onset of some types of PIOs can be recognized in the conceptual diagram in Figure 1, which depicts the phase lag between a pilot's control signal and a rate-saturated control surface response. While PIOs can be easily identified during post-flight data analysis, often pilots do not know they are in a PIO—from their perspective the aircraft appears to have broken.[17]

A. Contributing Factors to PIO

Three contributors must be present to induce a PIO; these contributors are the aircraft, the pilot, and the trigger. The aircraft can contribute to a PIO by having lags in the control system, unstable or marginally stable modes, slow actuators that cannot meet the demands of the pilot, or a combination of these factors. Pilots are the driving factor in a PIO, sustaining the oscillations by inputting higher than normal gain or leading signals to the control system.[17]

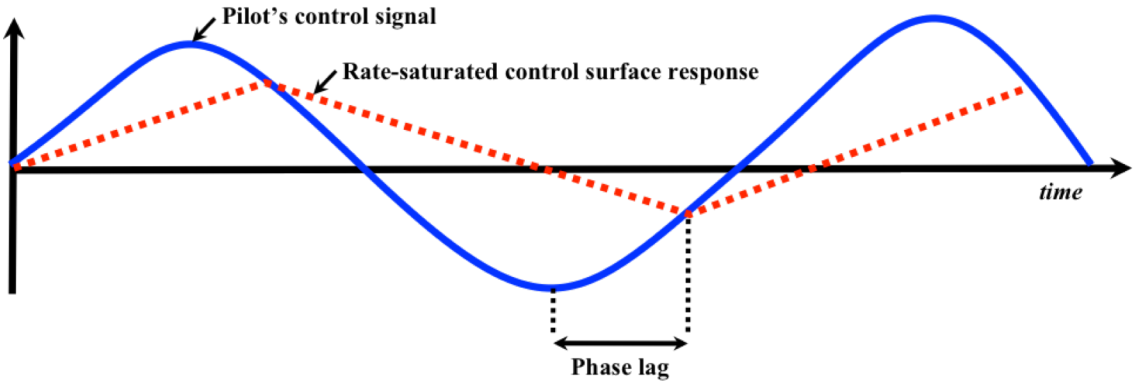

Figure 1. Diagram depicting phase lag between a pilot's control signal and a rate-saturated control surface response.

Finally, the piloted task or trigger is the impetus for increasing the pilot gain and starting the PIO. In PIO theory, the interplay between the aircraft, pilot and trigger has been broken down into two parts. One part is the interaction between the pilot and the trigger; the second part is between the pilot and the vehicle. These interactions are important to understanding when an aircraft may be vulnerable to a PIO.

1. Pilot-Trigger Interaction

A pilot flies an aircraft using one of two tracking methods. The first, and most common, is point tracking. In point tracking tasks, the pilot is attempting to track or converge on a point, such as the probe of an aerial refueling boom or the wingtip of the leader in formation flight. Maintaining an assigned altitude is another example of a point tracking task. As the pilot closes in on the desired point, the distances and associated time constants decrease. This leads to increased pilot gain and increased frequency of stick inputs required to track the desired point, which can trigger a PIO. For instance, when the pilot overshoots the nominal point, the resultant correction coupled with any vehicle latencies, leads to an overshoot in the opposite direction and the start of a PIO. The pilot is usually trained to go "hands off" and leave the control loop, ending the PIO.

The second tracking method that can trigger a PIO is boundary avoidance tracking (BAT). This usually occurs during landing or low altitude flight, but can occur in any situation where the pilot is stuck between two opposing boundaries (e.g. G-load, angle of attack (AoA), pitch/roll limits, or physical boundaries). As an example, if a nose-down gust hits the aircraft as it crosses the runway threshold, the pilot, to avoid damage from a ground strike, will pull the aircraft sharply up. Any latency in the system can cause the pilot to over-control. In this case, the overcorrection will lead the aircraft to rapidly approach the upper AoA boundary, which can be catastrophic at low altitude. The pilot would then push forward on the stick to stop the aircraft's movement towards the critical AoA, sending the nose towards the runway, setting off a PIO. In this case, the pilot is inclined to stay in the control loop, since a PIO is initially a better option then exceeding either boundary.

2. Pilot-Vehicle Interactions

Pilot-vehicle interactions are described by three categories of PIOs. In Category I PIOs, the vehicle characteristics are essentially linear, and the pilot behaves in a quasi-linear manner. The oscillations are caused by high open-loop gain. Category I PIOs are more repeatable, can be easily backed out of by the pilot, and are the least threatening.

A quasi-linear aircraft with rate or position limiting characterizes Category II PIOs. Additionally, nonlinearities such as stick command shaping or aerodynamics properties may also exist in a Category II PIO. The rate limiting of actuators can turn Category I PIO into a Category II by adding lag when there are large commanded inputs.

Category III PIOs are the result of serious nonlinearities within the aircraft system, such as mode switching in the software, or sudden hardware or aerodynamic changes. Category III PIOs can also result from a pilot switching tracking behaviors or input cues. PIOs in this category are always severe.

B. Link to Next Generation Aircraft Designs

PIO has been a problem for the entire history of controlled flight. While practical design considerations and analytical methods have been developed for PIO prevention, PIO events continue to occur during the initial flight-

testing of aircraft. Many design choices that enhance an aircraft's energy efficiency and environmental compatibility make the aircraft susceptible to PIOs.

Trends in next generation aircraft design relax stability requirements to gain improvements in energy efficiency and environmental compatibility through reduced drag. Traditional transport aircraft are designed to be stable, but these design choices are the result of compromises in the bare airframe that degrade the aircraft's energy efficiency and environmental compatibility.[1,2] Within a group of four aircraft design concept studies supported through NASA Research Announcements by the Subsonic Fixed Wing project of the NASA Aeronautics Research Mission Directorate's Fundamental Aeronautics Program, two of the concept studies demonstrate how stability requirements can continue to impose design constraints for next generation aircraft.[1,2] The remaining two concept studies identify relaxed static stability as a key fuel burn and cruise emissions technology.[3,4] Other concepts for next generation Blended Wing Body (BWB) aircraft take one step further with unstable aircraft designs augmented with closed-loop control to maintain stability,[5,6] as is done with modern fighter aircraft. This trend and example design concepts are shown in Figure 2.

As the trend in aircraft design leads to marginally stable or unstable but controllable airframes, high control power and feedback control augmentation are required to improve flying qualities and maintain closed-loop stability. In particular, best practices in PIO prevention recommend that an aircraft's actuation system exhibit

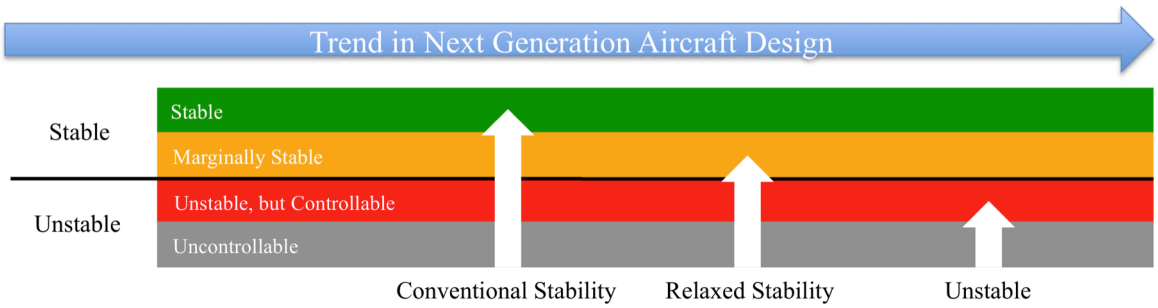

a) Diagram showing relationship next generation aircraft design trend and aircraft stability.

b) Next generation aircraft design concepts with conventional stability.[1,2]

c) Next generation aircraft design concepts with relaxed stability.[3]

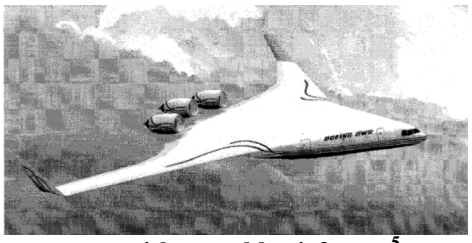

d) Next generation aircraft design concepts with unstable airframe.[5]

Figure 2. Trend for next generation aircraft towards relaxed stability and unstable designs.

sufficient rates and transient capability[17] as to avoid rate saturation of the surfaces, which is associated with Category II PIOs. Experience has shown that it is possible to equip unstable fighter aircraft with sufficient control power by using larger control surfaces and fast actuators. As the sizes of aircraft increase the moment forces needed from the control surfaces also increase, resulting in the need for larger control surfaces. Moving these large control surfaces at a high rate required to meet stability and control demands will necessitate larger hydraulic systems with higher power requirements. This poses a challenge for next generation transport and mobility aircraft.

For at least one next generation aircraft concept—the BWB configuration—the power required to move the control surfaces at a rate required for the stability and control of the vehicle has been termed technologically challenging due to the unprecedented horsepower requirements.[5] To supply the required power, BWB designers anticipate the need to extract secondary horsepower from the engines. Extraction of secondary horsepower will decrease the efficiency of the propulsion system and limit the design options for the system. For example, the power required is expected to exceed the power available from current turbofan engines and may exceed that available from advanced next generation engines. The only foreseeable solution by BWB designers is to design the aircraft to be stable at cruise, which reduces the rates and power required by the control surfaces. Doing so, however, threatens other design constraints and results in inefficient trim conditions at reduced lift and increased angle of attack.[6]

Subject to traditional design practices, the strive towards energy efficiency and environmental compatibility in combination with the complexity of new designs will inevitably increase the susceptibility of next generation aircraft to PIO events. Technology is needed to mitigate the effects of PIO factors and allow next generation aircraft to meet their potential in energy efficiency and environmental compatibility without abiding by constraining design practices.

III. Control Allocation technique to recover from Pilot Induced Oscillations (CAPIO)

CAPIO is designed to assist in the recovery from Category II PIOs that occur when control surfaces are operating at their maximum rate limit. Traditional control allocation techniques are susceptible to these Category II PIOs due to the phase lag between the desired and achieved rotational accelerations during rate limiting. CAPIO augments traditional control allocation techniques and seeks to reduce this phase lag and the associated risk of Category II PIOs.

Traditional control allocation systems seek to command control surface deflections to satisfy the desired rotational accelerations, denoted herein as v_d, from the stability and control augmentation system. The allocator commands a total control effort v, also referred to as the assumed achieved rotational acceleration in roll, pitch and yaw. For the purposes of the control allocation derivation, actuator dynamics are neglected and control surfaces are viewed as pure moment generators. These assumptions lead to the following approximate aircraft model

$$\dot{x} = Ax + B_u u = Ax + B_v v \qquad \text{Eq. 1}$$

$$v = Bu, \qquad \text{Eq. 2}$$

where x is the aircraft state vector of length $n \geq 3$, u is the control surface deflection vector of length $m > 3$, $B_u = B_v B$, and $B_v = \begin{bmatrix} I_{3x3} \\ 0_{(n-3)x3} \end{bmatrix}$.

Given the desired rotational accelerations requested by the control system, v_d, the control surface deflection is a solution to the system

$$Bu = v_d, \qquad \text{Eq. 3}$$

which is underdetermined. Standard non-iterative techniques can be used to solve Eq. 3 for a unique minimum-norm solution (see, e.g., Ref. 18, pp. 256-258). The imposition of bound constraints to ensure that the solution is within magnitude and rate limits, however, requires that the determination of the commanded control surface deflections be recast as an optimization problem.

The objective function of the optimization problem for the traditional control allocation system is represented by

$$J = \left\| W_P^{1/2}\left(Bu - v_d\right)\right\|_2^2 + \varepsilon\|u\|_2^2, \qquad \text{Eq. 4}$$

where the operation $\|\bullet\|_2^2$ is the square of the Euclidean norm and $\varepsilon > 0$. Simple bounds on u are imposed to ensure the solution is within magnitude and rate limits. The solution to this optimization problem, u^*, becomes the minimum norm solution to the system $Bu = v_d$ as ε approaches zero. While the solution u^* represents the desired actual control surface deflection, non-linear actuator dynamics represented by the actuator model $a(\bullet)$, which would require the determination of u_c such that $a(u_c) = u^*$, are ignored and the commanded control surface deflection, u_c, is set equal to u^*.

Under this allocation scheme, control surfaces functioning at their rate limit can lead to the assumed achieved rotational acceleration falling out of phase with the desired rotational acceleration. For example, this can happen when the desired rotational acceleration peaks and changes from increasing to decreasing, while the assumed achieved rotational acceleration may still be increasing to match the desired rotational acceleration (similar to Figure 1). In that case, the derivatives of the two signals have opposite signs and the result perceived by the pilot is a sluggish response.

CAPIO, in addition to minimizing the error between v (or Bu) and v_d, seeks to reduce phase lag by minimizing the error in the derivative of these signals. The objective function for CAPIO is represented by

$$J = \left\| W_P^{1/2}\left(Bu - v_d\right)\right\|_2^2 + \left\| W_D^{1/2}\left(B\dot{u} - \dot{v}_d\right)\right\| + \varepsilon\|u\|_2^2. \qquad \text{Eq. 5}$$

Similar to the optimization problem for the traditional control allocation system, simple bounds on u are imposed to ensure the solution is within magnitude and rate limits, and the solution to the control allocation problem, the commanded control surface deflection, u_c, is set equal to u^*.

The two weights, W_P and W_D, provide a manner in which CAPIO balances the objectives of having the control system follow the acceleration commands and their derivatives. In the application presented in this paper, W_P is always a positive constant and W_D is set either to zero or a positive constant value to disengage or engage the derivative following behavior of CAPIO. These two weights can also be utilized for axis prioritization.

Within CAPIO, two subsystems observe the signal dynamics of v and v_d to detect phase lag in real-time and determine when to engage or disengage derivative following. These subsystems are described in the next two subsections. The commanded control surface defections, which are solutions to the objective function in Eq. 5, are calculated on-line by a real-time optimizer. This real-time optimization is also described below.

A. Real-Time Detection of Phase Lag

Real-time detection of oscillatory behavior was designed into CAPIO to indicate when phase lag was present and needed to be addressed. The detection scheme used within the CAPIO system was a real-time reimplementation of what Mitchell and Hoh[19] developed for the PIO detector ROVER. Phase lag is detected based on the assumed achieved rotational accelerations, v, and the desired rotational accelerations, v_d. The calculated phase lag represents the phase lag apparent to the control allocation system, as seen in Figure 3 where v is calculated as $v = Ba(u_c)$ from the commanded control surface deflection u_c. As such, the calculated phase lag does not represent the phase lag experienced by the pilot.

Each of these signals are analyzed to identify peaks and compared to calculate the approximate phase difference. Peaks are identified by looking for zero crossings in the derivatives of the acceleration signals. The signals v and v_d are not filtered prior to calculating $\dot{v}$ and $\dot{v}_d$ to avoid introducing additional lag. To avoid the detection of false peaks due to noise, the magnitude of acceleration at a new peak is required to be outside of a deadband around the previous detected peak magnitude to be counted as a real peak. Additionally, peaks in the signal v must follow a peak in the signal v_d to ensure all calculated phase differences are positive.

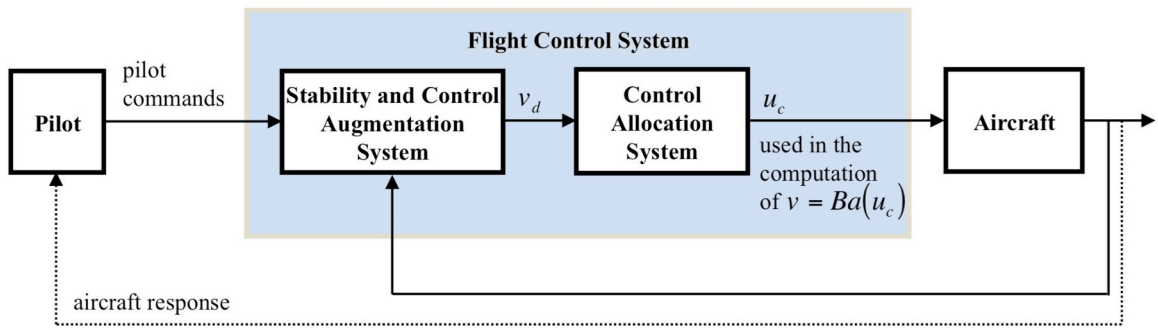

Figure 3. Conceptual system diagram.

The phase difference between v and v_d is calculated following the identification of a peak in v. To calculate the phase difference, the system assumes the signals exhibit sinusoidal behavior and have the same frequency. The frequency is calculated by treating the difference in time between the last two peaks of v_d as half of a period,

$$f = \frac{1}{2\left(t_{v_{d2}} - t_{v_{d1}}\right)}, \qquad \text{Eq. 6}$$

where $t_{v_{d1}}$ and $t_{v_{d2}}$ are the times of the last two peaks in v_d, as shown in Figure 4. Using this frequency, f, and the time, Δt, between the latest peaks of v and v_d, the phase difference $\Delta\varphi$ is calculated as

$$\Delta\varphi = 360 f \Delta t = 360\left(\frac{1}{2\left(t_{v_{d2}} - t_{v_{d1}}\right)}\right)\left(t_v - t_{v_{d2}}\right), \qquad \text{Eq. 7}$$

where t_v is the time of the latest peak in v.

This is done for the rotational accelerations in all three body-fixed axis. If the value of the phase difference in any axis is above a preset threshold, corresponding flags are sent to the subsystem of CAPIO that engages and disengages derivative following to indicate a significant phase lag is present in the system.

B. Derivative-Following Engagement and Disengagement

CAPIO balances two objectives: having the control system follow 1) the acceleration commands and 2) their derivatives. The derivative following behavior is engaged and disengaged through updates to W_D.

In theory, the derivative following mode is engaged any time a significant phase lag is detected and then

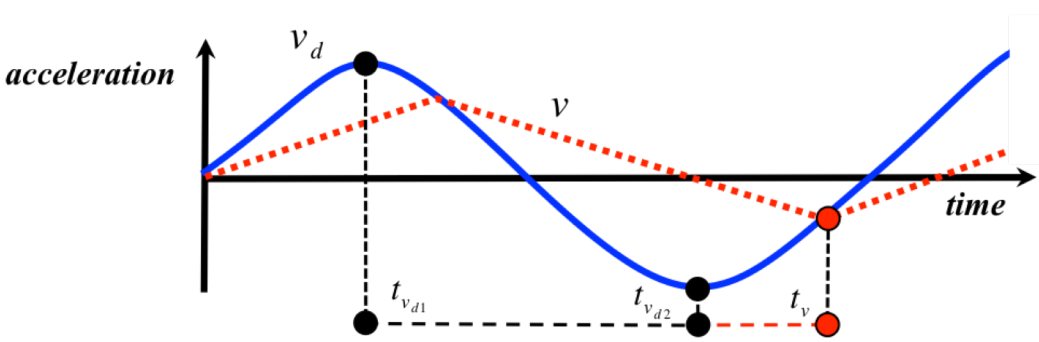

Figure 4. Phase lag detection diagram.

disengaged when the phase lag is no longer significant, based on the flag input from the real-time phase lag detector. The engagement and disengagement of the derivative following mode is done for each of the rotational axis individually, so significant phase lag in roll acceleration engages derivative following for the roll axis leaving the pitch and roll axes to follow accelerations. The derivative following mode causes W_D to increase from zero to a preset value that is determined by tuning. When W_D is sufficiently large, the second term in the objective function (Eqn. 5) becomes dominant, which forces the derivative of the assumed achieved accelerations to follow the derivative of the desired accelerations and eliminate the phase lag. When the phase lag drops below the preset threshold, W_D is set to zero.

In practice, there are certain situations when derivative following is not desired despite the detection of significant phase lag. The scenarios below outline exceptions used by CAPIO in determining when to engage and disengage derivative following.

1. Scenario One

One situation where CAPIO will disengage derivative following is when the desired acceleration levels off at a value in an asymptotic manner. Since no new peak is detected, a new phase difference cannot be calculated and derivative following will remain on, possibly with a large steady state error. To alleviate this, CAPIO looks at $\dot{v}_d$ and $\dot{v}$, and if the difference is below a threshold, derivative following is disengaged in that axis. This situation is illustrated in Figure 5.

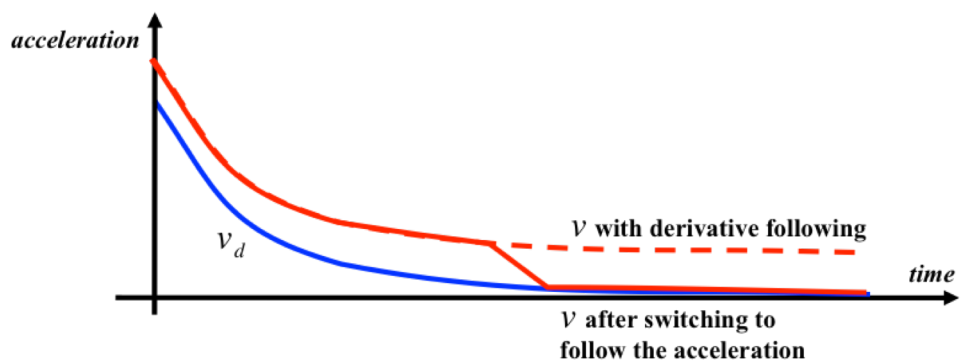

Figure 5. Situation when desired acceleration (v_d) levels off in an asymmetric manner.

2. Scenario Two

Another situation where CAPIO will disengage the derivative following exists when the stability and control augmentation system imposes maximum (or minimum) limits on the desired accelerations. If the desired acceleration is at a maximum (or minimum), the signal will flat-line and the derivative-following assumed achieved acceleration would also flat-line. This is a problem because the pilot will perceive the flat response as a loss in control power when requesting full control authority. CAPIO, therefore, will disengage derivative following if the desired acceleration is at a maximum (or minimum), as seen in Figure 6.

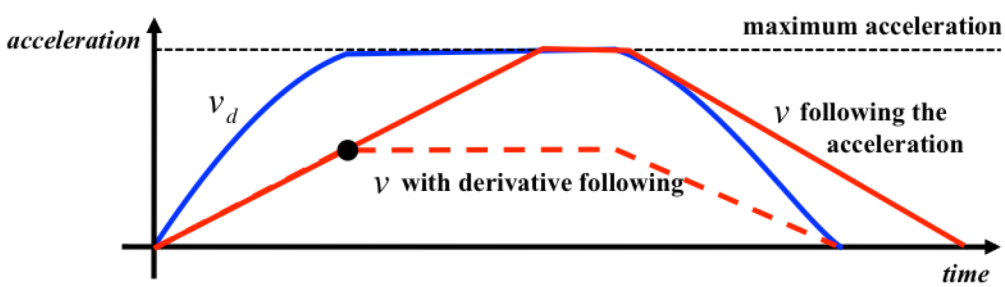

Figure 6. Situation when desired acceleration (v_d) is at a maximum limit.

3. Scenario Three

The final situation when CAPIO will not allow derivative following despite a flag from the phase lag detection subsystem is when the desired and assumed achieved accelerations have different signs. As illustrated in Figure 7, if the desired acceleration is positive and its derivative is near zero while the assumed achieved acceleration is still negative, the aircraft will accelerate in a direction opposite of the pilot's intentions. Pilots may interpret this response as a loss of control. To alleviate this problem, CAPIO will only allow derivative following when the desired and assumed achieved accelerations have the same sign.

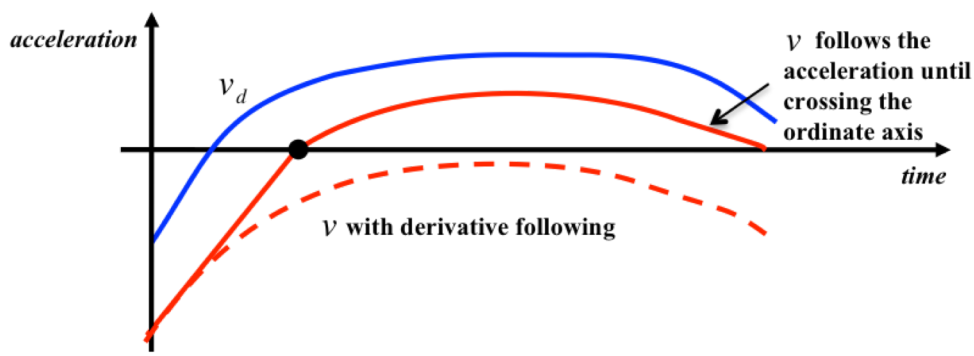

Figure 7. Situation when desired acceleration (v_d) and assumed achieved acceleration (v) have different signs.

C. Real-Time Optimization

CAPIO calculates the commanded control surface deflections using a real-time iterative optimization algorithm. Real-time optimization helps to ensure the efficient use of many multi-axis control surfaces such that together the surfaces provide sufficient control authority in each axis while balancing between v following v_d, and $\dot{v}$ following $\dot{v}_d$, with respect to the weighting matrix W_D.

For use in the real-time simulation environment, the optimal solution is computed at discrete times t_k. In this formulation, the variable u_k denotes the unknown column vector of desired actual control surface deflections at time t_k, and $\Delta t = t_k - t_{k-1}$. After eliminating the constant terms, the discrete objective function, based on Eq. 5, is given by

$$q(u_k) = \frac{1}{2} u_k^T H u_k + c^T u_k, \qquad \text{Eq. 8}$$

where the matrix H and the vector c are determined to be

$$H = 2\left(\Delta t^2 B^T W_P B + B^T W_D B + \varepsilon I\right) \qquad \text{Eq. 9}$$

$$c = -2\left(\Delta t^2 v_d{}^T W_P B + u_{k-1}{}^T B^T W_D B + \Delta t\, \dot{v}_d{}^T W_D B\right), \qquad \text{Eq. 10}$$

when $\dot{u}$ is approximated by $\dot{u} \approx (u_k - u_{k-1})/\Delta t$ and $\dot{v}_d$ is calculated as $\dot{v}_d \approx \left(v_{d_k} - v_{d_{k-1}}\right)\Big/\Delta t$. The solution u_k is the minimizer of $q\left(u_k\right)$ subject to bounds on u_k that ensure the solution is within magnitude and rate limits. These bounds take into consideration the actual achieved actuator positions at time t_{k-1}. If known, the actual control surface deflection can be sent as feedback to the control allocator. Otherwise, the actual control surface deflection can be approximated by a non-linear function a of the actuator model as $a\left(u_{k-1}\right)$. While the solution u_k represents the desired actual control surface deflection, non-linear actuator dynamics represented by the actuator model are

ignored and the commanded control surface deflection, u_c, is set equal to u_k.

The primary challenge with real-time optimization is to ensure satisfactory termination of the iterative process within the allowable time frame. Several steps are taken to meet this challenge. First, a first-derivative method is chosen in order to limit the complexity of each optimization iteration. Second, within the optimization method, advantage is taken of the fact that H is positive definite by using an exact line search (see, for example, Ref. 20, p. 21) instead of an iterative search. Third, explicit formation of H and c is avoided in the computation of $q(u_k)$ and $\nabla q(u_k)$. Instead, these computations are economized to take advantage of the outer product formulation of H and c.

The minimization of a quadratic function with positive definite Hessian can be accomplished by a variety of first-derivative optimization methods, though the stipulation of bounds narrows the field of choices. The optimization method selected was the Limited-memory BFGS Bound-constrained (L-BFGS-B) algorithm (see Ref. 21). An implementation of this method, available as open source Fortran code,[22] was integrated into the CAPIO algorithm. Only minor modifications were required to adapt L-BFGS-B to this context: L-BFGS-B was modified to perform an exact line search whenever possible, with a reduced number of function evaluations allowed prior to termination of the search; and a preset limit on the number of function evaluations was observed. At each frame, the optimizer used the solution of the last problem as its initial point. For more details on the implementation, see Ref. 23.

With this implementation, the simulation of the research aircraft math model with CAPIO was executed with an average increase in computational time per frame of only 17% relative to the math model without CAPIO. This outcome was sufficient to allow real-time execution of the CAPIO system at the required frame rate.

IV. Simulation Evaluation Description

The simulation evaluation was intended to assess the viability of CAPIO to enable reduced control surface rate requirements for energy-efficient next generation aircraft and identify areas of future research for the maturation of the technology. As such, the evaluation was designed to meet two objectives, as follows:

1) Demonstrate that CAPIO does not degrade system characteristics—measured by performance, Handling Qualities ratings and Pilot-Induced-Oscillations ratings—of a nominal aircraft.
2) Demonstrate that CAPIO improves system characteristics—measured by performance, Handling Qualities ratings and/or Pilot-Induced-Oscillations ratings—of an aircraft with reduced actuator rate limits when compared to a baseline control system.

Since the derivative following characteristics of CAPIO are activated after phase lag is detected, the point of interest is where flight control system commands to the aircraft exceed the control surface rate limits. To support this interest, the simulation evaluation required realistic motion cues for the pilots, a representative next generation research aircraft model, extreme research aircraft configurations, and demanding tasks. Details on these attributes, as well as the experimental procedure and data collected, are described below.

A. Vertical Motion Simulator Facility

The Vertical Motion Simulator is the ideal facility to test the CAPIO system because of its large motion envelope. Schroeder, *et. al.*[24] concluded that larger simulator motion envelopes provide more accurate HQR and PIO ratings than smaller simulator motion envelopes when compared to the same ratings taken in the actual aircraft. Schroeder also found that a large motion simulator was the only platform that induced markedly divergent PIOs. Additionally, pilots gave large motion higher confidence factor ratings and achieved lower touchdown velocities compared to small motion simulators.

The VMS motion system, shown in Figure 8, is an uncoupled, six-degree-of-freedom motion simulator. It is located in, and partially supported by, a specially constructed 120-ft tower. The VMS system motion capabilities are provided in Table 1.[25] Included in the table are two sets of limits: system limits that represent the absolute maximum levels of attainable under controlled conditions; and operational limits that represent attainable levels for normal piloted operations.

The cab, shown in white in Figure 8, serves as the aircraft cockpit. The

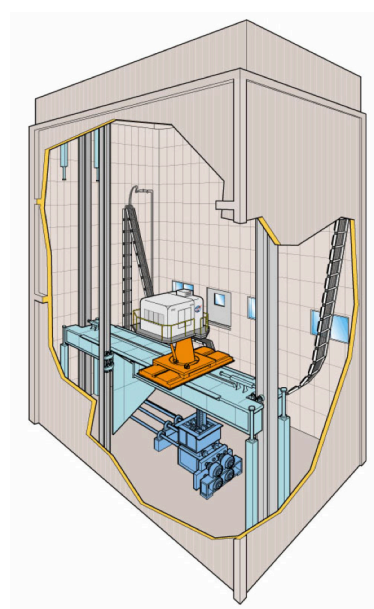

Figure 8. VMS facility.

evaluation pilot occupied the right seat, with the test engineer in the left. A computer image generation system creates the out-the-window visual scene for the six-window collimated display with the head-up display superimposed on the center window. Additional aircraft information was provided on three head-down displays at both pilot stations.

Table 1. VMS Motion System Performance Limits. [Ref. 25]

Degree of Freedom	Displacement		Velocity		Acceleration	
	System Limits	Operational Limits	System Limits	Operational Limits	System Limits	Operational Limits
Longitudinal	± 4 ft	± 4 ft	± 5 ft/sec	± 4 ft/sec	± 16 ft/sec^2	± 10 ft/sec^2
Lateral	± 20 ft	± 15 ft	± 8 ft/sec	± 8 ft/sec	± 13 ft/sec^2	± 13 ft/sec^2
Vertical	± 30 ft	± 22 ft	± 16 ft/sec	± 15 ft/sec	± 22 ft/sec^2	± 22 ft/sec^2
Roll	± 0.31 rad	± 0.24 rad	± 0.9 rad/sec	± 0.7 rad/sec	± 4 rad/sec^2	± 2 rad/sec^2
Pitch	± 0.31 rad	± 0.24 rad	± 0.9 rad/sec	± 0.7 rad/sec	± 4 rad/sec^2	± 2 rad/sec^2
Yaw	± 0.42 rad	± 0.24 rad	±0.9 rad/sec	± 0.8 rad/sec	± 4 rad/sec^2	± 2 rad/sec^2

B. Research Aircraft Model

The research aircraft math model flown in this evaluation was the Speed Agile Concept Demonstrator (SACD) – a short takeoff and landing (STOL) mobility concept being developed by industry under the U.S. Air Force Research Laboratory's (AFRL) Advanced Joint Air Combat System studies. The SACD program seeks to mature technology in the areas of high lift, efficient transonic flight, and flight control for future integrated mobility configurations that are intended to carry larger, heavier payloads than the C-130, fly efficiently across a wide range of speeds, cruise above Mach 0.8, and routinely operate from short, unprepared runways.[26] As part of the SACD program sponsored by the AFRL, an aircraft math model of the SACD and corresponding flight control system was developed and delivered to NASA.

The flight control system for the SACD model is a full-authority control system that accepts pilot inputs and calculates desired control surface deflections commands in order to stabilize, trim and maneuver the aircraft. The flight control system architecture is comprised of a stability and control augmentation system (SCAS) in series with a control allocation system, as shown in Figure 9. The SCAS calculates rotational acceleration commands in the aircraft's body-fixed axis. Next these commands are passed to the control allocation system, which calculates the necessary control surface deflections. The separation of the SCAS from the control allocation effectively decouples

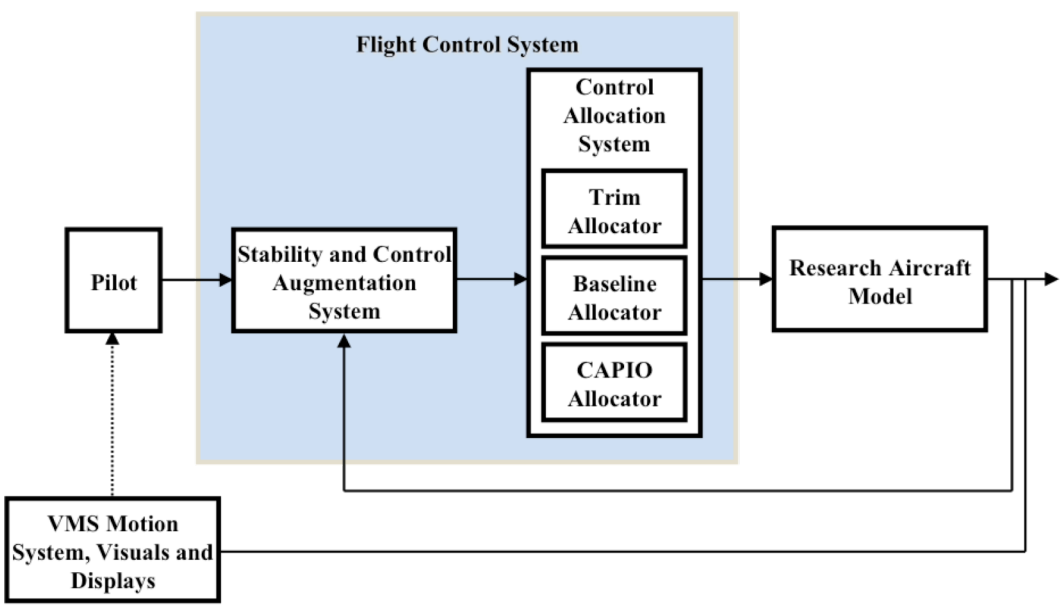

Figure 9. Flight control system diagram.

the two systems, allowing the two designs to mature independently such that changes can occur in one system without necessitating the redesign or retuning of the other system. For more information on the aircraft concept and flight control system, see Ref. 27 and 28.

For this simulation evaluation, the SCAS remained identical to the original system delivered and only the control allocation system was modified. The control allocation system is composed of three allocators with different functions and technology operating in parallel. The three allocators are the trim allocator, baseline allocator and CAPIO allocator. The purpose of the trim allocator is to determine the control surface deflections needed to achieve the trim commands. The purpose of both the baseline allocator and the CAPIO allocator is to determine the control surface deflections needed for stabilization and maneuvering. These latter two allocators are used interchangeably or together depending on a mode specified by the user. For example, the baseline allocator can be responsible for calculating the deflections needed for commands in all three axes while the CAPIO allocator is responsible for none, or vise versa; or the baseline allocator can be responsible for calculating the deflections needed for commands in one body-fixed axis while the CAPIO allocator is responsible for the remaining two body-fixed axes, or vise versa. Output signals from the trim allocator, baseline allocator and CAPIO allocator are merged and sent as one set of control surface deflection commands to the research aircraft math model.

C. Research Aircraft and Flight Control System Configurations

In order to support the research objectives of the evaluation, four configurations of the research aircraft and flight control system were flown for each task. The factors that differentiated the four configurations were the control allocator used and the rate limiting imposed on the control surfaces.

To recognize the impact CAPIO had on system characteristics, two versions of the control allocator were flown. The first version employed the baseline allocator in all axes and served as the reference for measuring performance. The second version, referred to as the CAPIO allocator, employed the CAPIO allocation algorithm in the pitch and roll axes, with the baseline allocator operating in the yaw axis. Pitch and roll were the axes of interest in the two piloted simulation tasks described in the following subsection.

The control surface rate limits were set at a nominal value and a reduced value for actuators in the axis of interest for each task. The reduced actuator rates were chosen such that actuators would encounter their limits to accomplish the task. This would introduce phase lag that would induce PIO tendencies, thus providing sufficient differences in system characteristics between the nominal and reduced rate limited aircraft configurations.

Table 2 summarizes each of the resulting sets of configurations for each task. Other factors, such as the atmospheric conditions, initial location, and trim airspeed, varied by task but remained consistent across each of a task's four configurations.

Table 2. Research Aircraft and Flight Control System Configurations.

Configuration					Task	
Name	Control Allocation System			Actuator Rate Limit in Axis of Interest	Offset Approach and Landing	Boundary Avoidance Tracking
	Roll Axis	Pitch Axis	Yaw Axis			
Baseline 100	Baseline	Baseline	Baseline	100°/s	✓	✓
CAPIO 100	CAPIO	CAPIO	Baseline	100°/s	✓	✓
Baseline 25	Baseline	Baseline	Baseline	25°/s	✓	
CAPIO 25	CAPIO	CAPIO	Baseline	25°/s	✓	
Baseline 40	Baseline	Baseline	Baseline	40°/s		✓
CAPIO 40	CAPIO	CAPIO	Baseline	40°/s		✓

D. Piloted Simulation Tasks

Two pilot-in-the-loop tasks were designed and deployed in this simulation to engage the pilot-aircraft system in high-gain, precision maneuvers to expose any PIO tendencies in the system in a controlled and repeatable manner. The two tasks were offset approach and landing task and a pitch boundary avoidance tracking task.

1. Offset Approach and Landing Task

The offset approach and landing (OA&L) task was designed to assess handling qualities and reveal PIO

tendencies in the lateral axis under tight, aggressive control. To accomplish this objective, pilots were asked to land the airplane given drastic situational circumstances and demanding performance standards. The task began with the aircraft configured in a trimmed approach descending through cloud cover, which obscured the pilot's view of the runway. While the glideslope and localizer indicated a proper approach, the aircraft was offset 300 feet laterally and 300 feet longitudinally; this scenario represented a simulated navigational equipment failure. At 230 feet above ground level (AGL), the aircraft broke out of the cloud ceiling and the pilot had to locate the runway. The pilot was then required to maneuver the aircraft through moderate turbulence and attempt to land within a touchdown box painted on the runway. The pilot was expected to fly the aircraft in a manner that met specific performance standards. The performance standards for the precision landing at touchdown were longitudinal distance from the threshold, lateral offset from runway centerline, deviation from runway heading and track, deviation from target airspeed, and sink rate.

2. Boundary Avoidance Tracking Task

The boundary avoidance tracking (BAT) task was designed to become progressively harder and expose PIO tendencies in the longitudinal axis as the pilot's control gain increased with the task difficulty. The task was defined by two pairs of magenta needles arranged similar to a tic-tac-toe board on the Primary Flight Display (PFD), which are shown in Figure 10. The needles formed a square, and the pilot was required to keep the bore-sight of the aircraft within this square as it moved up and down. The vertical motion of the square followed a sum-of-sines pattern, which repeated itself every 30 seconds. As the pattern repeated, the size of the square shrunk by 25%. The goal was to keep the bore-sight of the aircraft within the square as long as possible, and the task was terminated when the bore-sight encountered the square's boundary. Since the square was continuously moving and the atmospheric condition included light turbulence, the task required pilots to actively control the aircraft to avoid the boundaries. For more details on the implementation of the BAT task, see Ref. 29. The criteria used to measure the performance during the BAT task was the length of time spent in flight before the bore-sight encountered the square's boundary.

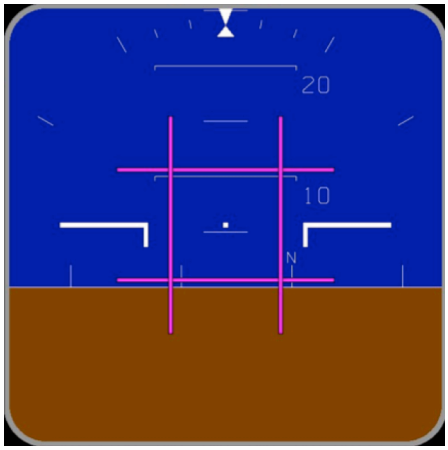

Figure 10. PFD displaying BAT task.

E. Experimental Procedure

The simulation was conducted over the course of two weeks. During those two weeks, seven test pilots participated in the study. The pilot schedule allotted two days for each pilot to complete the test matrix, with a maximum of two pilots per day, alternating sessions to reduce pilot fatigue. Time at the conclusion of the matrix was reserved for repeat sessions to be used at the discretion of the research engineers.

Orientations were held to brief each pilot on the experiment's background, objective, tasks, procedures and aircraft system. For each task, pilots were allowed one one-hour warm-up session, and prior to collecting data for each configuration, a series of practice runs was conducted until the pilots felt they were achieving consistent results. Following the practice runs, a minimum of three data runs were flown for each configuration. At the conclusion of each practice and data run, performance feedback was provided to the pilot via an end-of-run display in the cockpit. Subjective and objective data was collected throughout and upon the completion of the data runs, as described in the following subsection.

Each pilot flew and evaluated all four configurations for both tasks at least once, resulting in a comprehensive data set representing over 350 data runs. The pilots were not told what configuration they were flying.

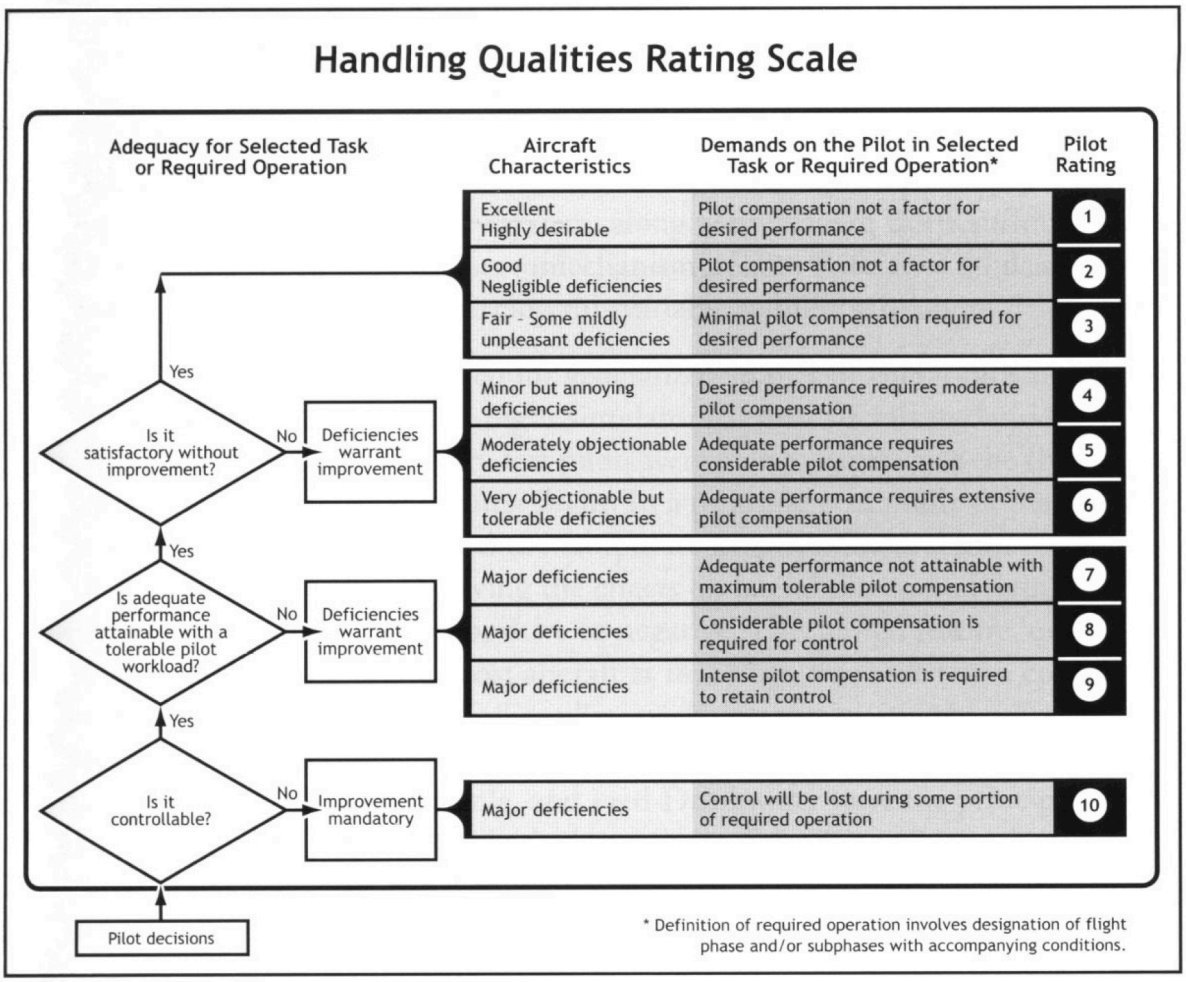

Figure 11. Cooper-Harper Handling Qualities rating scale

F. Collection of Objective and Subjective Data

Both objective and subjective data were collected during the simulation evaluation. The objective data recorded digitally during the simulation evaluation was in three formats. These formats include the simulation time history data with performance standard data, end-of-run pilot displays, and video with audio recording. The subjective data collected for each configuration, when appropriate, was in the form of Handling Qualities Ratings, PIO ratings, and pilot comments.

The Handling Qualities Ratings (HQR) were collected with the Cooper-Harper Handling Qualities Rating Scale[16] shown in Figure 11. The HQR scale provides numerical data on how the pilot perceived the required workload and aircraft performance for a given task. Specific performance standards and metrics are required to provide a HQR, so the scale was only appropriate for, and ratings were only collected for, the offset approach and landing task.

The PIO ratings were captured with the PIO rating scale[16] shown in Figure 12. The PIO scale provides a numerical rating meant to reflect the pilot's perception of the aircraft's performance and flight characteristics for a given task with particular attention on oscillation and undesirable motion.

Verbal comments expressed by pilots were recorded and written comments were captured on pilot comment cards unique to the task. These comments provide insight into how each pilot viewed the task and perceived the system's overall performance.

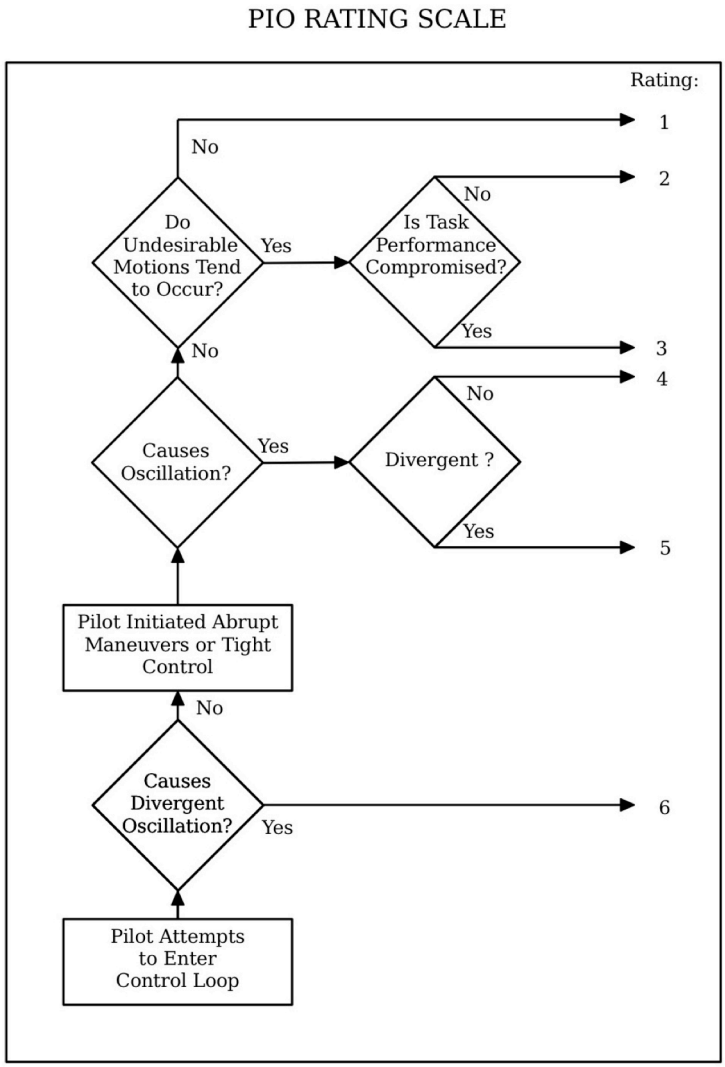

Figure 12. PIO rating scale.

V. Evaluation Results and Discussion

The results of the motion-based piloted simulation conducted in the VMS are presented and discussed with respect to the research objectives.

A. Simulation Results in the Presence of PIOs

Analysis of the simulation data revealed that CAPIO contributed to a reduction in the severity and duration of PIOs, and to an improvement in the pilots' perception of PIO tendencies and in the pilots' PIO ratings, as compared to the baseline allocator. This benefit is particularly pronounced for the aircraft configuration with reduced actuator rate limits.

1. Post-Simulation Identification of PIOs

PIOs experienced during the simulation were identified visually by analyzing plots of the simulation data. The signals reviewed were the inputs used by CAPIO to detect a phase lag in the system. These signals were v_d, the desired rotational accelerations, and v, the assumed achieved accelerations. Roll axis and pitch axis components of these signals were investigated for the offset approach and landing task and the boundary avoidance tracking task, respectively. The system was declared to be in a PIO when two criteria were met: First, three or more peaks must be observed in the assumed achieved acceleration signal, with the peak size greater than twenty percent of the maximum amplitude. Second, there must be a visibly significant phase lag between the desired acceleration and the following assumed achieved acceleration signals. For each PIO identified, the number of peaks and their duration were measured. These measurements were started at the second of the consecutive peaks since a single peak does not qualify as a PIO.

2. Offset Approach and Landing Task Results

While the system with nominal rate limiting experiences few PIOs, the system with reduced actuator rates was susceptible to oscillatory behavior at two points during the task: upon breakout below the ceiling when the pilot first banks after visually identifying the runway, and during final alignment with the runway when the pilot inputs a roll reversal. Since CAPIO does not prevent the occurrence of PIOs (but rather helps the recovery), PIOs are seen at both susceptible points for the baseline and CAPIO allocators with reduced actuator rates. When the PIOs occur, however, the average number of peaks per PIO reduces from 8.1 peaks with the baseline allocator to 5.2 peaks with the CAPIO allocator. The average duration of PIOs also reduces from 8.0 seconds with the baseline allocator to 4.9 seconds with the CAPIO allocator. This shows that PIOs stop sooner with the CAPIO allocator as compared to the baseline allocator. Similar improvements are present for the nominal rate limiting configurations based on data from the few PIOs that did occur. Results are shown in Figure 13 and Figure 14.

Pilots' perception of the PIO tendencies and their PIO ratings are consistent with the improvements in the

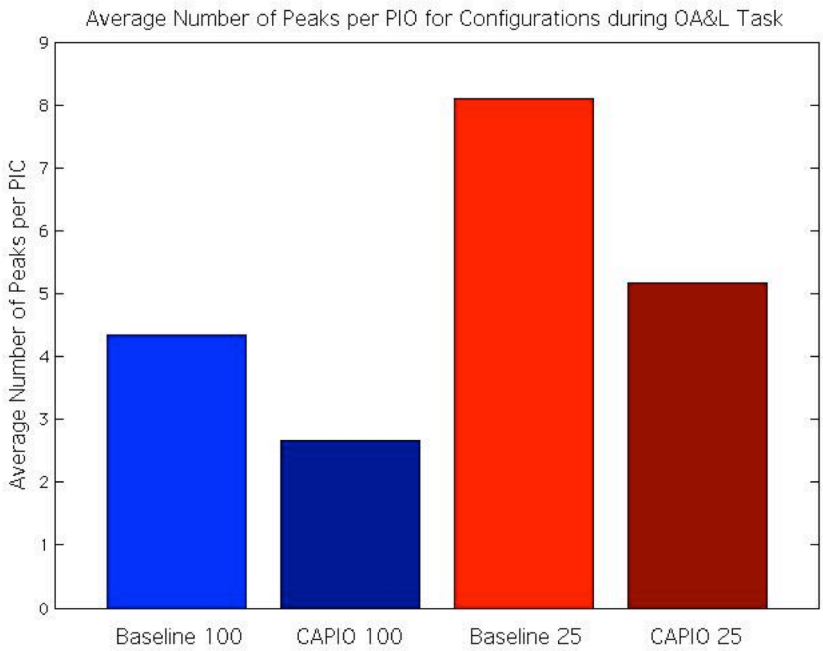

Figure 13. Average number of peaks per PIO during the OA&L task.

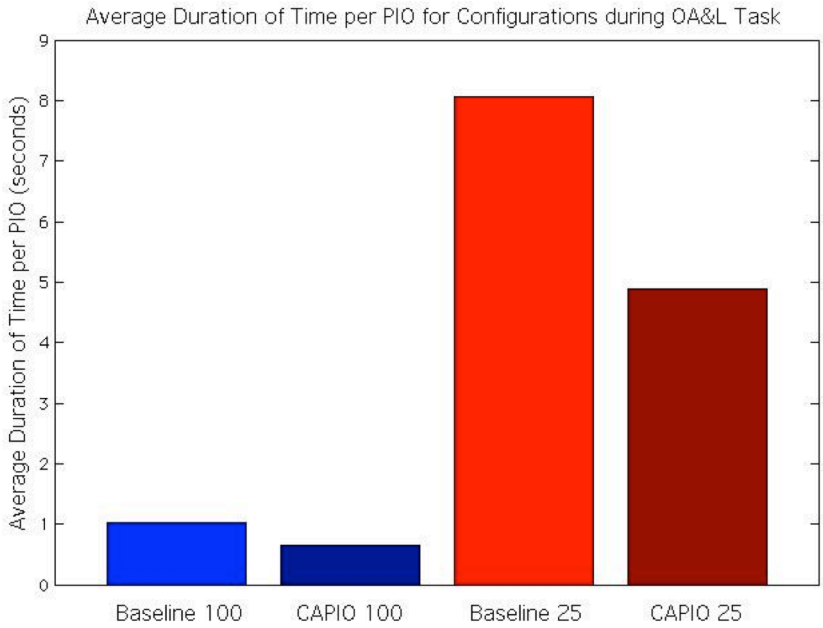

Figure 14. Average duration of PIOs during the OA&L task.

severity and duration of PIOs identified in the simulation data. With reduced actuator rate limits, pilots indicated fewer PIO tendencies for the CAPIO allocator after flying the offset approach and landing task—over half of the pilots indicated PIO tendencies in roll with the baseline allocator but only about a quarter of pilots indicated PIO tendencies in roll with the CAPIO allocator. The plot showing the average pilot perception of PIO tendencies is given in Figure 15.

The pilots' PIO ratings are given in Figure 16. Each column represents a configuration and the colors of the bar represent the percentage of rating values received from pilots. The majority of pilots gave the systems with nominal actuator rate limits a PIO rating of one, corresponding to the observation that no undesirable motions tended to occur. When actuator rate limits were reduced, only approximately a third of ratings were a value of one. More than 60% of the PIO ratings for the baseline allocator configurations were 4, corresponding to the observation of non-divergent oscillations as a result of abrupt maneuvers or tight control. The PIO ratings for the CAPIO allocator configurations was better with only approximately 20% of the ratings being 4 and over a third of the ratings being 3, corresponding to the observation of undesirable motions that compromised task performance.

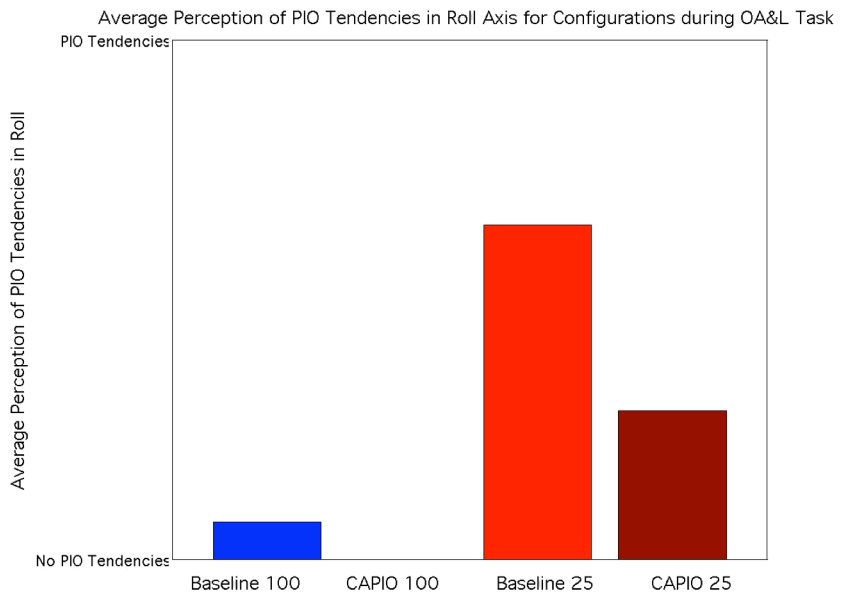

Figure 15. Average pilot perception of PIO tendencies in roll axis during the OA&L task.

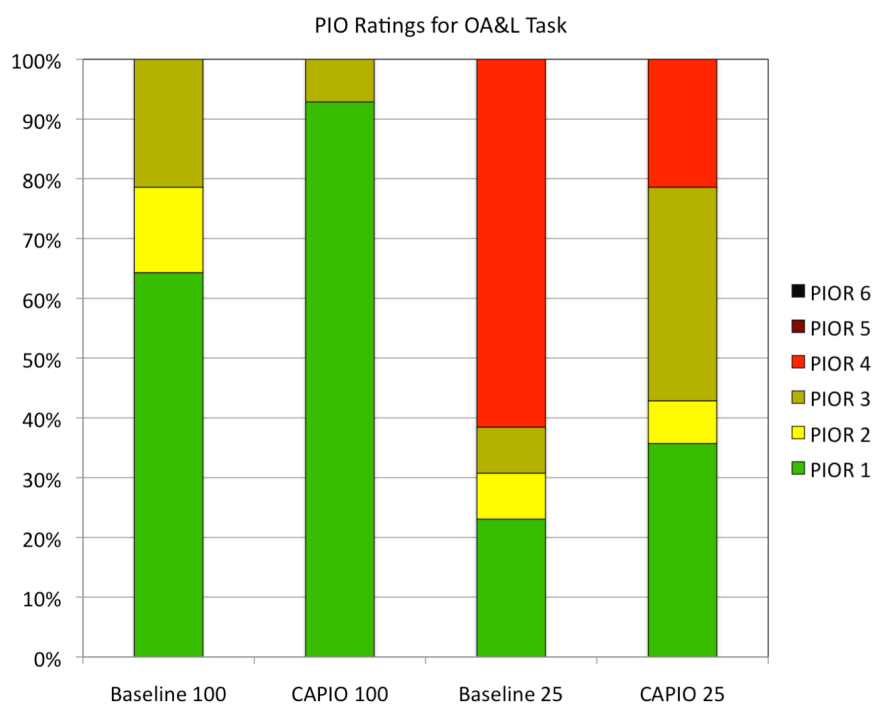

Figure 16. PIO ratings for the OA&L task.

3. Boundary Avoidance Tracking Task Results

Due to the continuous demands imposed by the BAT task, PIOs were experienced throughout the simulation runs. When a PIO was experienced, the average number of peaks per PIO and average duration of time spent in the PIO reduced with the CAPIO system for aircraft configurations with both actuator rate limits as shown in Figure 17 and Figure 18.

The CAPIO allocator helps the system to recover from the PIOs quickly, as compared to the baseline allocator, but in consequence the system has more opportunity to enter another PIO. This is seen in the number of PIOs per minute of simulation run time with the reduced actuator rate. The configuration with the baseline allocator on average enters 3.4 PIOs per minute of simulation run time while the configuration with the CAPIO allocator enters 3.7 PIOs per minute of simulation run time on average. Despite the increase in the number of PIOs with CAPIO, the overall result is still an overall reduction of PIO behavior shown by a smaller percentage of time spent in PIO. On average for nominal rate limiting configurations, the percentage of time spent in PIO reduced 55% between the baseline and CAPIO allocators. The configurations with reduced actuator rate limits also show the percentage of time spent in PIO reduced 46% between the baseline and CAPIO allocators.

In Figures 19, 20 and 21, time histories of the aircraft signals with reduced actuator rate limits are presented for an example BAT run. Specifically, Figure 19 shows the desired and assumed achieved rotational accelerations, Figure 20 shows pilot stick position in the longitudinal direction together with aircraft pitch rate, and Figure 21 presents BAT task boundaries and pitch angle of the aircraft. The signals are acquired from the same simulation run and are plotted without axis values to conceal details of the research aircraft model.

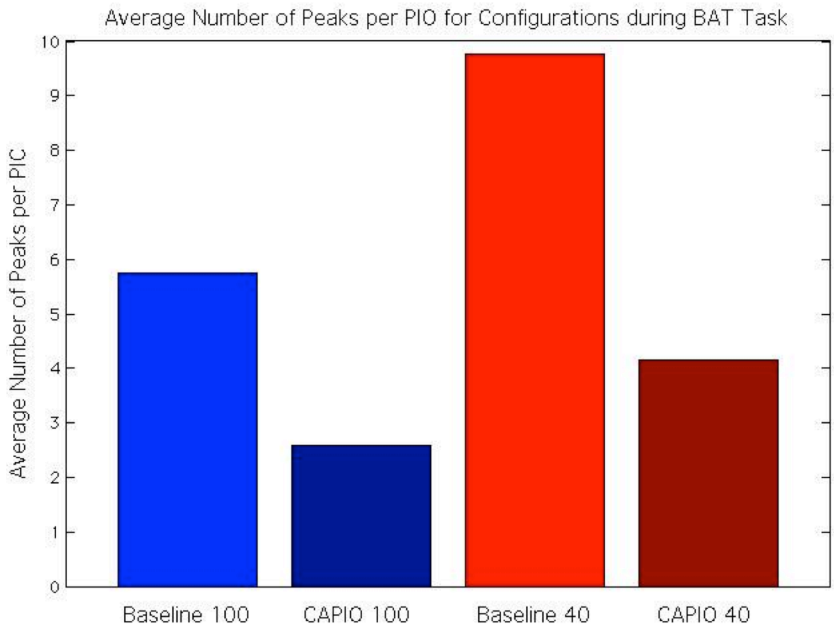

Figure 17 . Average number of peaks per PIO during the BAT task.

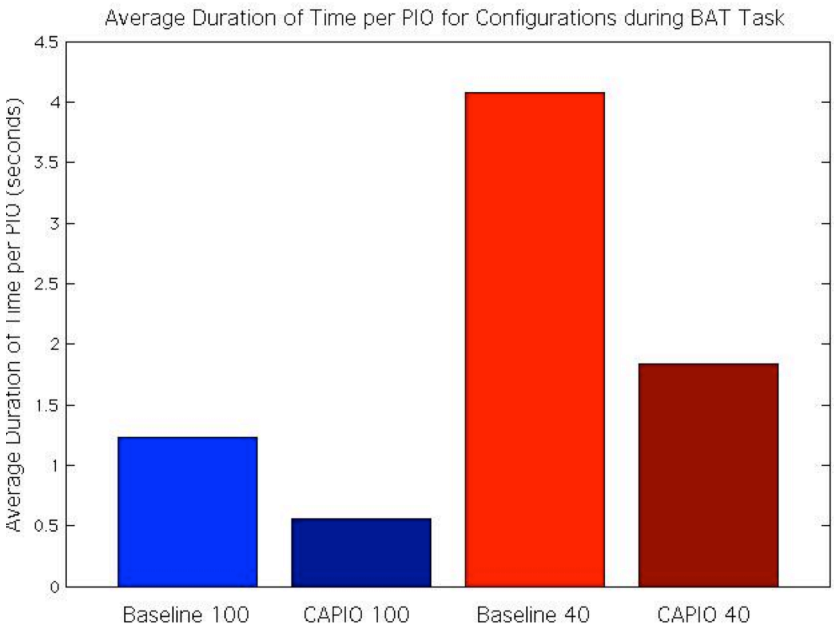

Figure 18. Average duration of PIOs during the BAT task.

The example time history data of the desired and assumed achieved accelerations in Figure 19 shows that while the number of PIOs increased with the CAPIO allocator at reduced actuator rate limits, the severity and duration of the PIOs were worse with the baseline actuator. The configuration with the baseline allocator experiences two PIOs starting at approximately 8 and 24 seconds and the configuration with the CAPIO allocator experiences eight shorter PIOs starting at approximately 6, 14, 17, 19, 27, 30, 33 and 36 seconds. At these times, approximately 90° phase shift between the stick position and pitch rate for the reduced rate limit configurations confirms that the oscillations in the desired and assumed achieved accelerations are, in fact, PIOs. The trace of the BAT boundaries and pitch angle of the aircraft provide context for the task that the pilot-aircraft-control system was attempting to execute.

Improvements in the oscillatory behavior led to improved performance during the boundary avoidance tracking task measured by the length of time spent in flight before the bore-sight encountered the square's boundary. Regardless of the aircraft's actuator rate limits, CAPIO extended the average time before encountering the boundary. With both nominal rate limits and reduced rate limits, CAPIO improved the time to failure by approximately 18% over the baseline allocator.

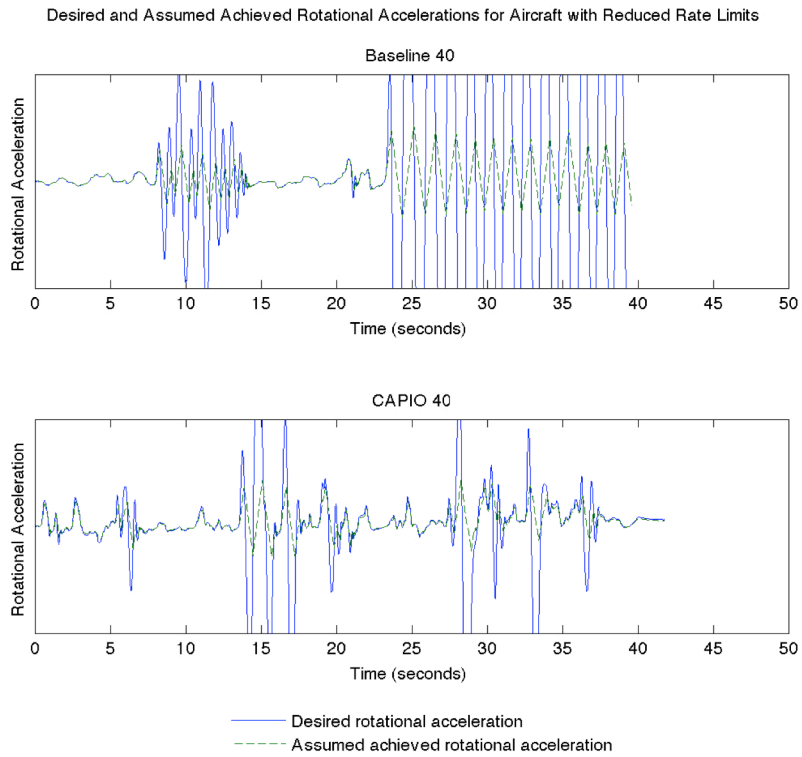

Figure 19. Desired and assumed achieved rotational acceleration for the aircraft with reduced rate limits.

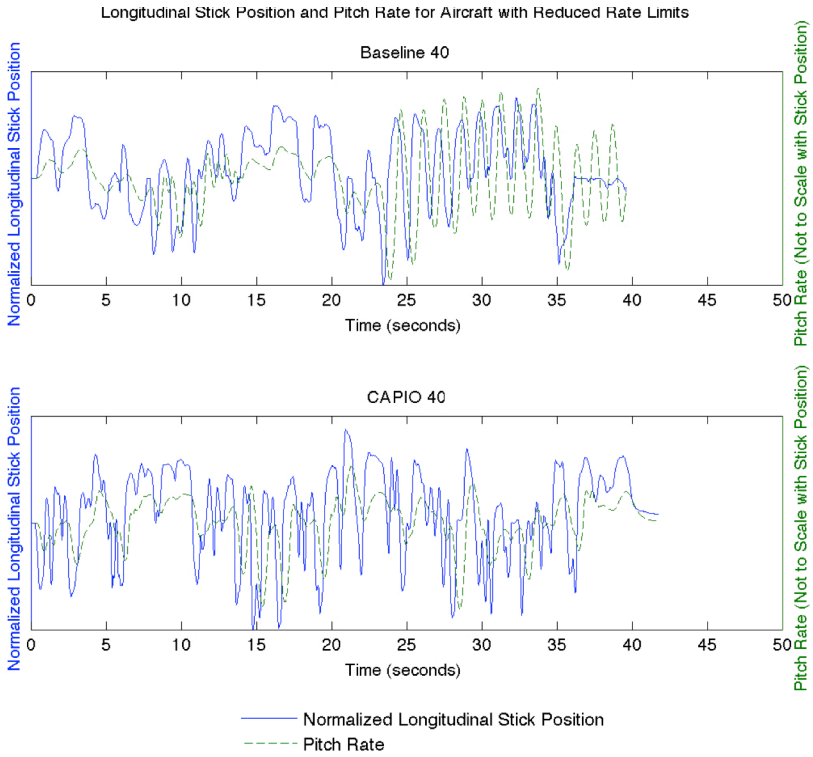

Figure 20. Pilot stick position in the longitudinal direction and aircraft pitch rate for the aircraft with reduced rate limits.

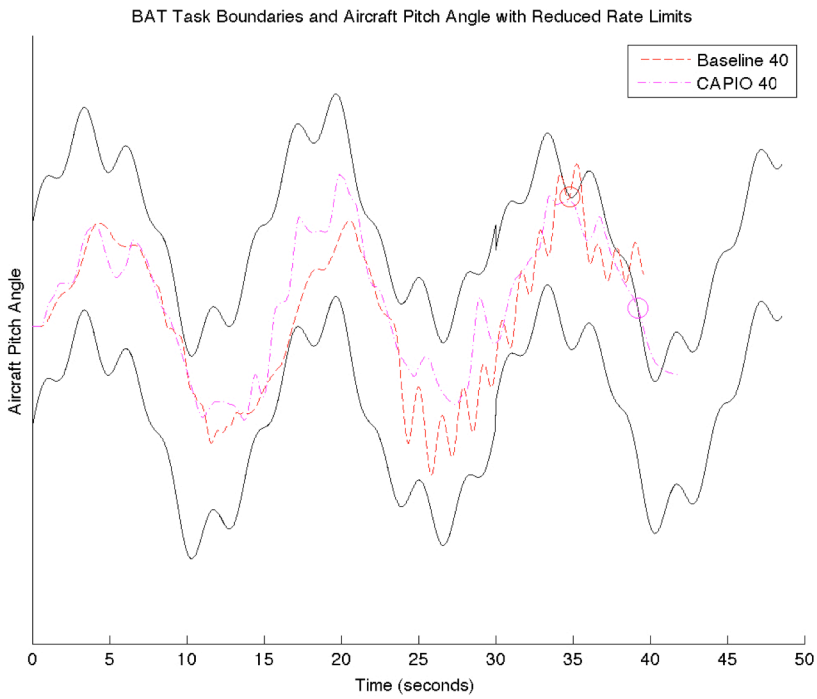

Figure 21. The BAT task boundaries and pitch angle of the aircraft with reduced rate limits.

Pilots' perception of the PIO tendencies and their PIO ratings are mostly consistent with the improvements in the severity and duration of PIOs identified in the simulation data. The plot showing the average pilot perception of PIO tendencies is given in Figure 22. With reduced actuator rate limits, pilots indicated fewer PIO tendencies for the CAPIO allocator; all of the pilots indicated PIO tendencies with the baseline allocator but only about three quarters of pilots indicated PIO tendencies with the CAPIO allocator. This trend changes, however, with the nominal actuator rates. In this case, over half the pilots indicated PIO tendencies for the baseline allocators and one additional pilot indicated PIO tendencies for the CAPIO allocator. Pilot comments do not explain why this pilot indicated PIO tendencies for the system with nominal actuator rates and the CAPIO allocator, but not for the system with nominal actuator rates and the baseline allocator. The pilot's learning curve and familiarity with the task may have influenced the rating as the configuration with nominal actuator rates and the CAPIO allocator was the first

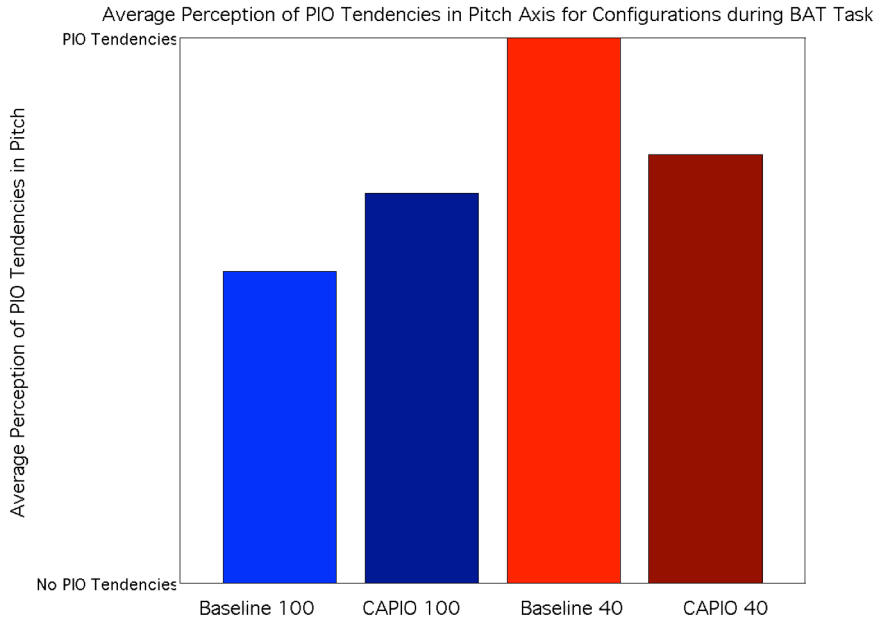

Figure 22. Average pilot perception of PIO tendencies in pitch axis during the BAT task.

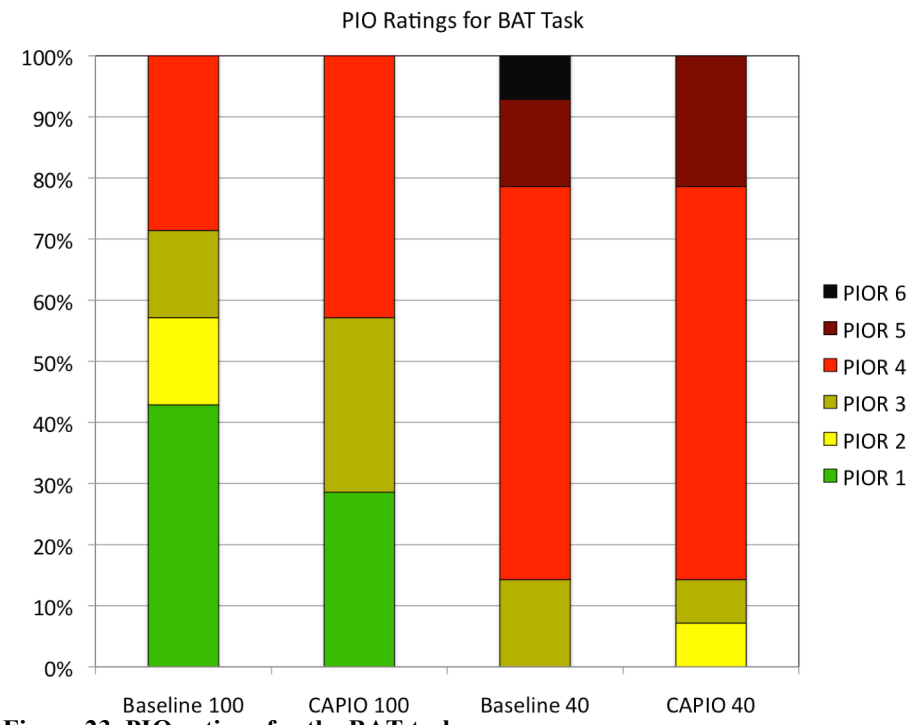

Figure 23. PIO ratings for the BAT task.

configuration flown by the pilot for the boundary avoidance tracking task and the configuration with nominal actuator rates and the baseline allocator was the last configuration flown. PIO behavior during the pilot's data runs are consistent with averages presented earlier for these configurations; the pilot experienced one PIO for each of the configurations with nominal actuator rates and the number of peaks was smaller and duration of the PIO was shorter with the CAPIO allocator.

The pilots' PIO ratings are given in Figure 23. The PIO ratings range 1 to 4 for both systems with nominal actuator rate limits. Similar to the perceived PIO tendencies, the system with nominal actuator rate limits received worse ratings for the CAPIO allocator with fewer ratings of 1 and more ratings of 4 than the baseline allocator. In this case, two pilots rated the system with the CAPIO allocator worse and, again, it is suspected that the pilots' learning curve and familiarity with the task may have influenced the rating since the configuration with nominal actuator rates and the CAPIO allocator was the first configuration flown by both pilots for the boundary avoidance tracking task and the simulation data shows an improvement in PIO behavior with the CAPIO allocator during the pilots' data runs. At the reduced actuator rate limits, the majority of PIO ratings were four with both allocators but the configuration with the CAPIO allocator received slightly better ratings. The best rating for this configuration was 2, corresponding to the observation of undesirable motion that did not compromise task performance, and the worst rating was 5, corresponding to the observation of divergent oscillations as a result of abrupt maneuvers or tight control. For the configuration with the baseline allocator at the reduced rate limits, the best rating was 3 and the worst rating was 6, corresponding to the observation of divergent oscillation as a result of the pilot attempting to enter the control loop

B. Simulation Results of Overall System Characteristics

Analysis of the simulation data revealed that the overall system characteristics were strongly influenced by the control surface rate limits. The baseline allocator and CAPIO allocator received comparable overall pilot assessment for both the offset approach and landing task and the boundary avoidance tracking task, as well as comparable Handling Qualities ratings and task performance for the offset approach and landing task.

1. Offset Approach and Landing Task

Pilot comments captured on the pilot comment cards convey that flight dynamics of the system degrade as control surface rate limits are reduced. For the nominal aircraft configuration, the pilots on average declared the ability to control and track bank angle to be fair and the ability to correct lateral offset to be between fair and difficult. With the rate limits reduced, the average pilot rating for both of these characteristics dropped to difficult. This degradation is present regardless of the control allocator. The average predictability of roll response ranges between satisfactory and unsatisfactory, with a slight decrease towards unsatisfactory for configurations with reduced actuator rate limits. The difference in predictability offered by the CAPIO and baseline allocator, however, is not significant. Pilot comments indicate that the sluggish response or lag in response from the systems contributes to the unpredictability, especially at reduced actuator rate limits.

The distinction between the nominal aircraft and the aircraft with reduced actuator rate limits is also prominent in the Cooper-Harper ratings. The nominal aircraft had mostly Level 2 handling qualities for either allocator given a majority of Cooper-Harper ratings of 4, 5 and 6. At these ratings, pilots found the system deficiencies to range from minor but annoying to very objectionable but tolerable due to the extensive compensation required. Based on pilot comments collected during the simulation, it was found that the difficulty of the task contributed to the need for extensive compensation and poor system rating. The handling qualities for the aircraft with reduced actuator rate limits were worse at mostly Level 3, given a majority of Cooper-Harper ratings of 7, 8 and 9. (See Figure 24.) The reduced actuator rate limits imposed another challenge on the pilots in addition to the difficult task, resulting in a system that pilots deemed to have major deficiencies.

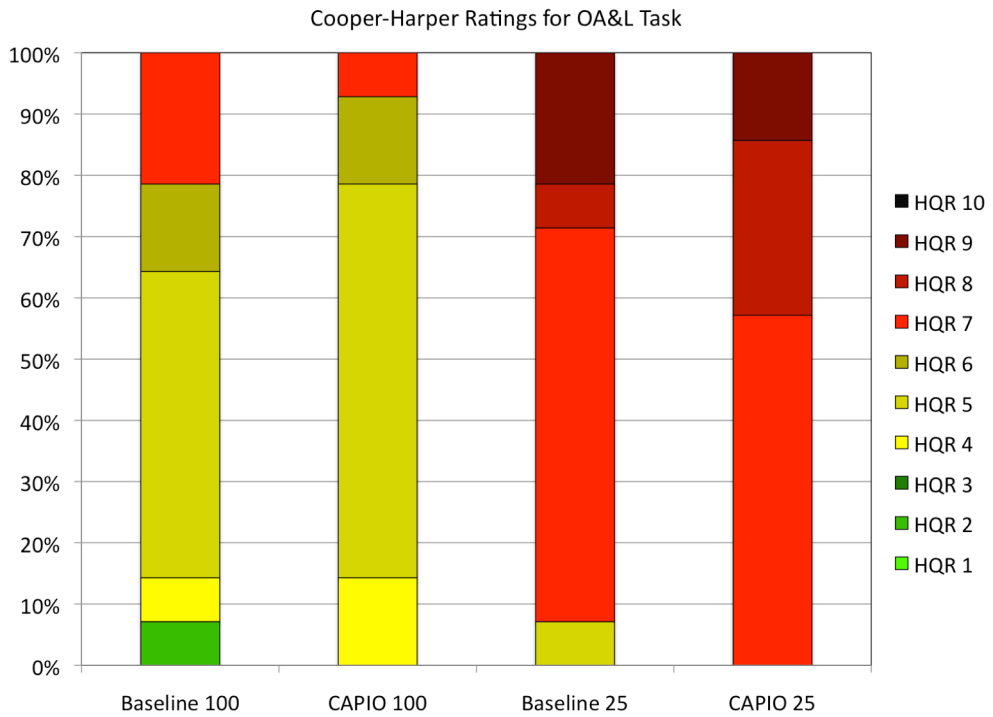

Figure 24. Cooper-Harper HQRs for configurations during the OA&L task.

Despite the poor handling qualities ratings and pilot comments, on average pilots achieved performance within the desired and satisfactory performance standards threshold for the final approach and touchdown. The desirable and satisfactory performance is achievable because, for all configurations, pilots were able to retain tight control over the system by operating at very high workloads and recovering from oscillatory behavior immediately prior to touchdown.

2. Boundary Avoidance Tracking Task

Pilot comments captured on the pilot comment cards for the boundary avoidance tracking task also convey that flight dynamics of the system degrade as control surface rate limits are reduced. For the nominal aircraft configuration, the pilots on average declared the ability to control and track pitch to be fair. With the rate limits reduced, the average pilot rating for the ability to control and track pitch dropped to between fair and difficult. This degradation is present regardless of the control allocator. The average predictability of pitch response ranges between satisfactory and unsatisfactory, with a slight decrease towards unsatisfactory for configurations with reduced actuator rate limits. The difference in predictability offered by the CAPIO and baseline allocator, however, is not significant. As seen for the offset approach and landing task, pilot comments for the boundary avoidance tracking task indicate that the sluggish response or lag in response from the systems contributes to the unpredictability, especially at reduced actuator rate limits.

C. Summary Observation

The simulation evaluation was intended to assess the viability of CAPIO to mitigate the effects of factors that make next generation aircraft more susceptible to PIOs as airframe designs become more energy efficient. In particular, the simulation evaluation assessed the effects of reducing actuator rate limits. As the actuators of the aircraft functioned at their reduced rate limits, phase lag was introduced. In Ref. 16, McRuer has linked phase lag to

poor pilot ratings. The experimental results are consistent with expectation, revealing degradation in pilot ratings from the configuration with nominal actuator rate limits to the configuration with reduced actuator rate limits. While CAPIO was meant to reduce the phase lag, it was designed to only do this after significant phase lag was detected. Due to this design feature, CAPIO did not impact the overall pilot perception.

This experiment did validate that CAPIO helped to reduce PIO behavior introduced by control surface rate limiting, and that pilots recognized the improvement in their ability to maintain or regain closed-loop control of the aircraft with respect to PIO behavior. CAPIO accomplished this by adjusting the control allocation mode in flight, causing changes in the effective vehicle dynamics that can be expected to degrade pilot perceptions.[16,17] Since pilot perception of overall system characteristics remained consistent between the baseline and CAPIO allocators, it appears that the changes in the effective vehicle dynamics caused by mode switching in CAPIO did not adversely impact pilot perception. This result also suggests that the real-time optimization algorithm used within CAPIO offered similar control performance to the baseline allocator, which did not use real-time optimization.

In summary, the simulation evaluation effectively meet the research objectives by demonstrating that CAPIO does not degrade system characteristics of a nominal aircraft, and that CAPIO improves PIO recovery characteristics of an aircraft with reduced actuator rate limits when compared to the baseline control allocator.

VI. Conclusion

A motion-based, piloted simulation evaluation was completed to assess the impact of the CAPIO allocator on the pilot-aircraft-control system characteristics. The simulation evaluation represents a milestone following a two-year effort by NASA and NASA contractors to mature CAPIO from TRL 1 to TRL 5. CAPIO is intended to address problems that arise from stringent actuator rate limits for multi-input, multi-output applications, such as phase lag and PIOs. The system does this by actively detecting and eliminating phase lag introduced by control surface rate limiting. Results from the simulation evaluation confirm that CAPIO successfully contributed to a reduction in the severity and duration of PIOs, and to an improvement in the pilots' perception of PIO tendencies and in the pilots' PIO ratings, as compared to the baseline allocator. Since CAPIO is currently only designed to improve system characteristics after phase lag is detected, it received a comparable overall pilot assessment, as well as comparable Handling Qualities ratings and task performance for the offset approach and landing task, to the baseline allocator.

Even with the accomplishments from the simulation evaluation, further maturation of CAPIO is still needed to enable lowering the actuator rate limit requirements. Analytical studies are needed to enhance and guarantee the closed-loop stability properties of an aircraft, and to extend CAPIO to influence and improve overall system characteristics. The system integration and impact of CAPIO will also need to be demonstrated through piloted flight studies. If successful, CAPIO will allow aerodynamically efficient airframe designs that are currently unattainable due to technologically prohibitive control power requirements.

Acknowledgments

This research was accomplished with the contributions of many individuals and organizations. The authors thank our project pilot and coauthor, Gordon H. Hardy, for his guidance throughout the research and evaluation of CAPIO. In addition to Gordon H. Hardy, the authors thank the pilots who participated in and provided insight during the preliminary and final simulation evaluations, including Dana Purifoy, Richard Ewers and Jim Smolka from NASA Dryden Flight Research Center, MAJ Carl Ott from the Army Aeroflightdynamics Directorate, Dan Dugan from NASA Ames Research Center, Jim Lindsey from Monterey Technologies Inc. at NASA Ames Research Center, Jim Martin and George Tucker. The authors are also thankful for the exceptional service and assistance provided by the NASA Ames Research Center VMS team. Finally, the authors extend their appreciation to two projects within the NASA Aeronautics Research Mission Directorate – the Fundamental Aeronautics Program's Subsonic Fixed Wing Project and the Integrated Systems Research Program's Environmentally Responsible Aviation Project – for their support of this research.

References

[1] Greitzer, E. M., Bonnefoy, P. A., De la Rosa Blanco, E., Dorbian, C. S., Drela, M., Hall, D. K., Hansman, R. J., Hileman, J. I., Liebeck, R. H., Levegren, J., Mody, P., Pertuze, J. A., Sato, S., Spakovszky, Z. S., Tan, C. S., Hollman, J. S., Duda, J. E., Fitzgerald, N., Houghton, J., Kerrebrock, J.L., Kiwada, G. F., Kordonowy, D., Parrish, J. C., Tylko, J., Wen, E. A., Lord, W. K., "N3 Aircraft Concept Designs and Trade Studies, Final Report," NASA/CR-2010-216794/VOL1, December 2010

[2] Bruner, S., Baber, S., Harris, C., Caldwell, N., Keding, P., Rahrig, K., Pho, L., Wlezian, R., "NASA N+3 Subsonic Fixed Wing Silent Efficient Low-Emissions Commercial Transport (SELECT) Vehicle Study," NASA/CR-2010-216798, November 2010

[3] Bradley, M. K., Droney, C. K., "Subsonic Ultra Green Aircraft Research: Phase I Final Report," NASA/CR-2011-216847, April 2011

[4] D'Angelo, M. M., Gallman, J., Johnson, V., Garcia, E., Tai, J., Young, R., "N+3 Small Commercial Efficient and Quiet Transportation for Year 2030-2035," NASA/CR-2010-216691, May 2010

[5] Cameron, Douglas and Princen, Norman, "Control Allocation Challenges and Requirements for the Blended Wing Body," *AIAA Guidance, Navigation and Control Conference and Exhibit*, AIAA, Denver, Colorado, August 2000, AIAA-2000-4539

[6] Roman, D., Allen, J. B., and Liebeck, R. H., "Aerodynamic Design Challenges of the Blended-Wing-Body Subsonic Transport," *AIAA Applied Aerodynamics Conference*, AIAA, Denver, Colorado, August 2000, AIAA-2000-4335

[7] Durham, W. C., Bordignon, K. A., "Multiple Control Effector Rate Limiting," *Journal of Guidance, Control and Dynamics*, Vol. 19, No. 1, January-February 1996, pp. 30-37

[8] Bodson, M., "Evaluation of Optimization Methods for Control Allocation," *Journal of Guidance, Control and Dynamics*, Vol. 25, No. 4, July-August 2002, pp. 703-711

[9] Oppenheimer, M. W., Doman, D. B., "A Method for Including Control Effector Interactions in the Control Allocation Problem," *AIAA Guidance, Navigation and Control Conference and Exhibit*, AIAA, Hilton Head, South Carolina, August 2007, AIAA-2007-6418

[10] Frost, S. A., Bodson, M., Acosta, D. M., "Sensitivity Analysis of Linear Programming and Quadratic Programming Algorithms for Control Allocation," *AIAA Infotech@Aerospace Conference and AIAA Unmanned… Unlimited Conference*, AIAA, Seattle, Washington, April 2009, AIAA-2009-1936

[11] Yildiz, Y., Kolmanovsky, I. V., "A Control Allocation Technique to Recover from Pilot-Induced-Oscilaltions (CAPIO) due to Actuator Rate Limiting," *2010 American Control Conference*, Baltimore, Maryland, June-July 2010

[12] Yildiz, Y., Kolmanovsky, I. V., Acosta, D., "A Control Allocation System for Automatic Detection and Compensation of Phase Shift Due to Actuator Rate Limiting," *2011 American Control Conference*, San Francisco, California, June-July 2011

[13] Yildiz, Y., Kolmanovsky, I., "Stability Properties and Cross-Coupling Performance of the Control Allocation Scheme CAPIO," *Journal of Guidance, Control, and Dynamics*, Vol. 34, No. 4, July-August 2011, pp. 1190-1196

[14] AGARD-AR-279, Advisory Group for Aerospace Research and Development, "Handling Qualities of Unstable Highly Augmented Aircraft," Advisory Report No. 279, May 1991

[15] MIL-HDBK-1797, Department of Defense Handbook, "Flying Qualities of Piloted Aircraft," December 1997

[16] McRuer, D., "Pilot-Induced Oscillations and Human Dynamic Behavior," NASA Contractor Report 4683, July 1995

[17] "Flight Control Design Best Practices," Research and Technology Organization, North Atlantic Treaty Organization, Neuilly-sur-Seine Cedex, France, December 2000, RTO-RT-29

[18] Golub, G. H., and Van Loan, C. F., *Matrix Computations*, 2nd ed., The John Hopkins University Press, Baltimore, Maryland, 1989

[19] Mitchell, D. G., and Hoh, R. H., "Development of Methods and Devices to Predict and Prevent Pilot Induced Oscillations," SBIR Phase II Report, AFRL-VA-WP-TR-2000-3046, December 2000

[20] Fletcher, R., *Practical Methods of Optimization*, 2nd ed., John Wiley and Sons, Chichester, New York, 1987.

[21] Byrd, R. H., Lu, P., Nocedal, J., and Zhu, C., "A limited memory algorithm for bound constrained optimization", SIAM Journal on Scientific Computing 16 (1995), pp. 1190--1208.

[22] Zhu, C., Byrd, R. H., Lu, P., Nocedal, J., "Algorithm 778: L-BFGS-B: FORTRAN Subroutines for Large Scale Bound Constrained Optimization", ACM Transactions on Mathematical Software, 23 (1997), pp. 550--560.

[23] Leonard, M., "Real-Time Optimization for use in a Control Allocation System to Recover from Pilot Induced Oscillatons," *AIAA Guidance, Navigation, and Control Conference*, AIAA, Boston, Massachusetts, August 2013

[24] Schroeder, J. and Chung, W., "Simulator Platform Motion Effects on Pilot-Induced Oscillation Prediction" Journal of Guidance, Control, and Dynamics, Vol. 23, May-June 2000

[25] Aponso, B., Beard,S., Schroeder, J., "The NASA Ames Vertical Motion Simulator – A Facility Engineered for Realism," Royal Aeronautical Society Spring 2009 Flight Simulation Conference, London, UK, 3-4 June 2009

[26] Broad Agency Announcement by the Air Force Research Laboratory, Air Vehicles Directorate, Aeronautical Sciences Division, AFRL/VAAA, Speed Agile Concept Demonstration, Number 07-07-PKV

[27] Hyde, D. C., Shweyk, K. M., Brown, F., Zeune, C., "Flight Control Development for a Speed-Agile Powered-Lift Transport Aircraft," *AIAA Atmospheric Flight Mechanics Conference*, AIAA, Minneapolis, Minnesota, August 2012, AIAA-2012-4578

[28] Shweyk, K. M., Hyde, D. C., Levengood, K., Zeune, C., "Validation of the Flight Control System of a Conceptual, Powered-Lift, Speed-Agile, Transport Aircraft," *AIAA Atmospheric Flight Mechanics Conference*, AIAA, Minneapolis, Minnesota, August 2012, AIAA-2012-4579

[29] Craun, R. W., Acosta, D. M., Beard, S. D., Hardy, G. H., Leonard, M. W., Weinstein, M., "Boundary Avoidance Tracking for Instigating Pilot Induced Oscillations," *AIAA Atmospheric Flight Mechanics Conference*, AIAA, Boston, Massachusetts, August 2013